A method for modeling a common-mode impedance for the AC motor

Houcine Miloudi, Abdelber Bendaoud, Mohamed Miloudi

APELEC Laboratory, University of Sidi Bel Abbès, Algeria
E-mail: el.houcine@yahoo.fr, abdelber.bendaoud@univ-sba.dz, mohamed.miloudi@univ-sba.dz,

Abstract. The paper proposes a frequency method to identify the components of an unknown three-phase AC motor considered as a magic box operating in a high-frequency range. A mathematical model of the AC motor is suitable for prediction and analysis of a common-mode (CM) current and Electromagnetic Interference (EMI) problems in a cable-fed motor-driven system. The parameters of the proposed model are defined by the frequency method using a CM impedance measurement. The proposed method can be used to predict and solve complex electrical systems, study high-frequency problems, and design the EMI component to improve Electromagnetic Compatibility (EMC).
The Agilent 4294A Impedance Analyzer is used to measure the frequency-domain characteristic impedance of the AC motor. The measured results basically verify the extracted data, while the discrepancy between the measured and simulated results is also analysed.

Keywords: AC motor, Common Mode (CM), high frequency, identification method, transfer function.

Metoda za modeliranje sofazne impedance motorja

V prispevku je predstavljena metoda za analizo trifaznega izmeničnega motorja. Matematičen model motorja je primeren za analizo sofaznih tokov in elektromagnetne interference na električnih povezavah. Parametri predlagane metode so definirani s frekvenčno metodo z meritvijo sofazne impedance. Predstavljeno metodo lahko uporabimo za reševanje kompleksnih električnih sistemov, visokofrekvenčno analizo in načrtovanje komponent za izboljšanje elektromagnetne skladnosti. Meritve karakteristične impedance izmeničnega motorja smo izvedli z impedančnim analizatorjem Agilent 4294A. Analizirali smo tudi razliko med izmerjenimi rezultati in rezultati simulacij.

1 INTRODUCTION

Any mathematical model can be obtained either by a theoretical approach based on physical laws or by an experimental approach based on system measurements [1].

When designing of an electrical, control or other analogue system, it is usually necessary to work with the frequency-dependent transfer functions and impedances, and to construct the Bode's diagrams.

In this study we proposed an approach to predict the transfer function of a three-phase AC motor operating in a high-frequency (HF) range. We deal with the problem of building a mathematical model of a dynamic system based on the motor data in tow configurations, CM and DM mode, and set up an experimental modelling method. The proposed approach is valid for any physical model.

HF modelling of an induction machine is addressed in many papers [2, 3, 4, 5, 6, 7, 8, 9, and 18]. The proposed model is widely used in EMC studies. For example, to design and determine the importance of conducted and radiation emissions in adjustable-speed driven systems used in industrial applications, electrical vehicles or electrical airplanes, it is necessary to have a sufficiently accurate model of the various components constituting the entire system. The AC motor is one of them. Using the system identification method which is based on the frequency response of a linear dynamic model shows how the model reacts to sinusoidal inputs. If input u(t) is sinusoidal of a certain frequency, then the output y(t) will also be a sinusoidal. However the input amplitude and phase will be different. This frequency response is most often depicted by two plots; one showing the amplitude change as a function of the sinusoidal frequency and one showing the phase shift as a function of the frequency. This is known as the Bode's plot.

In this work the system is identified from the frequency response of the AC motor. To describe the impedance of the AC motor only the magnitude plot is needed, whereupon the transfer-function parameters of the motor can verified by the second curve, i.e the phase plot. The motor is thus considered as a magic box. Based on the frequency response, we can find its transfer function in the frequency range from 100 Hz to 30 MHz.

2 THEORETICAL APPROACH

The Bode's plot is a plot of the magnitude and phase of the transfer function or some other complex-valued magnitude versus the frequency (s = jw) [3].

Two plots – both have the frequency logarithm on the x-axis
- The y-axis magnitude of the transfer function, H(s), in logarithmic axes (or decibels).
- The y-axis phase angle in radium/second using semi-logarithmic axes.

The transfer function can be defined as [3]:

$$G(s) = \frac{Y(s)}{X(s)} \qquad (1)$$

The roots of polynom X(s) are called poles of the system and the roots of Y(s) are called zeros of the system [3].

Though, the real electrical systems are usually complex, there are also some that are simple, i.e : the integrator, first-order and, second order systems.

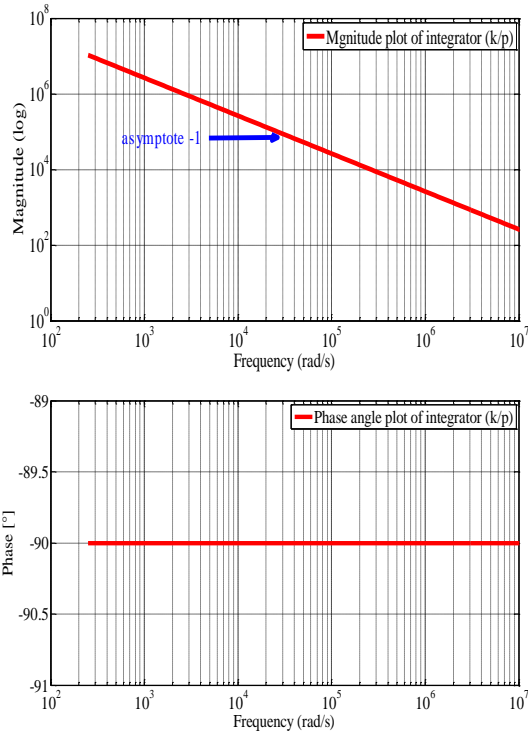In this theoretical approach we present only the system transfer functions in a CM impedance model.

Figure 1. Frequency response of the integrator.

2.1 Integral system:

The magnitude of the integrator transfer function is:

$$Z_{CM1} = \frac{K}{S} \qquad (2)$$

The phase of the integrator transfer function is:

$$\phi = -\tan^{-1}\left(\frac{w}{0}\right) = -\frac{\pi}{2} \qquad (3)$$

Fig.1 shows that in the plot on the log-log graph, the magnitude plot is linear and its slope is -1. For all frequencies, the phase shift is a constant, -90°.

2.2 Second-order system

The differential equation describing the system is of the second order :

$$B_2 \frac{d^2 s(t)}{dt^2} + B_1 \frac{d\ s(t)}{dt} + B_0 s(t) = A_0 e(t) \qquad (4)$$

The transfer function of the second-order system can be evaluated as the frequency by relation [4]:

$$H(s) = \frac{A_0}{B_2 s^2 + B_1 s + B_0} \qquad (5)$$

$$w_n = \sqrt{\frac{B_0}{B_2}} \qquad (6)$$

w_n is the undamped natural frequency

$$\zeta = \frac{B_1}{2\sqrt{B_0 B_2}} \qquad (7)$$

where ζ is the damping ratio.
The magnitude of the transfer function is:

$$Z_H = \frac{k}{\left[\ (\frac{1}{w_n^2})\ s^2 + \frac{2 \cdot \xi}{w_n}\ s + 1\ \right]} \qquad (8)$$

The phase angle of the second-order system is:

$$\varphi_H = -arctg\left(\frac{2 \cdot \xi\ \cdot \frac{w}{w_n}}{1 - (\frac{w}{w_n^2})^2}\right) \qquad (9)$$

Fig. 2 shows the frequency response of the second-order system for the magnitude and phase angle of H(s).
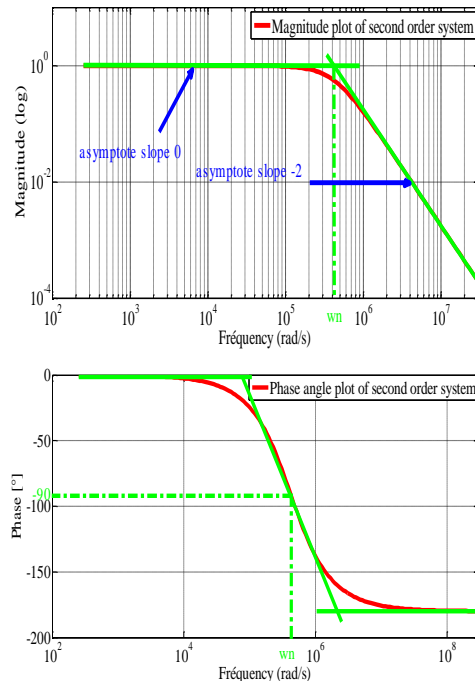

Figure 2. Frequency response of the second-order system.

The approximative amplitude plot consists of two straight lines; one line lies along slope (0) when $w << w_n$ and one along slope -2 when $w >> w_n$.

The approximative phase angle of complex poles and zeros consist of three straight lines; the first is at zero frequency $w \rightarrow 0$, the second is at $-90°$ at corner frequency w_n and the third at -180° close to large frequency $w \rightarrow +\infty$.

3 AN IDENTIFICATION METHOD FOR THE AC MOTOR CM IMPEDANCE

The ratio of CM voltage $V_{CM}(s)$ to CM current $I_{CM}(s)$ signal, where the input is sinusoidal, is expressed as Z_{CM} (jω) of the transfer function of the CM impedance of the AC motor given by the following relation [6]:

$$Z_{CM}(s) = \frac{V_{CM}(s)}{I_{CM}(s)} \qquad (10)$$

Construction of the transfer function from the Bode's plot using the extraction measurement data follows the below steps:

First, the model impedance is measured with an impedance bridge (HP4294A). The parameter is obtained by a CM test. Its configuration is shown in Fig. 3.
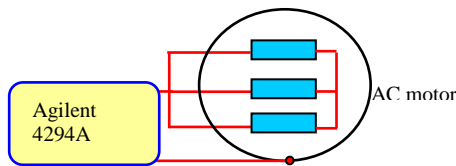

Figure 3. CM test configuration [13].

Evolution of the motor CM impedance with the magnitude being the function of the frequency is represented in Fig. 4.
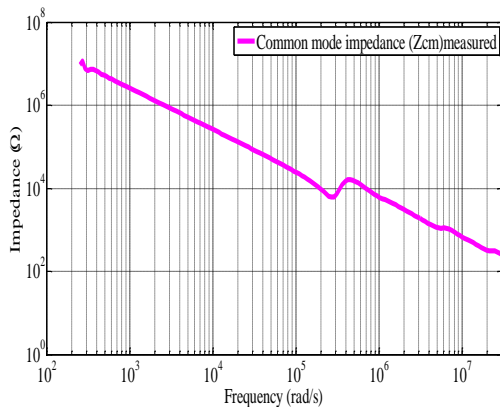

Figure 4. Measured impedance (magnitude) of the AC motor.

Gain Z_{CM} (jw) of the gain curve as a function of frequency w, can be approximated piecewise by straight lines with integer slopes. Each of them can be easily shown on a logarithmic plot. The entire Bode's log magnitude plot of Z_{CM} is obtained by superpositioning the straight lines.

3.1 Identification of the transfer function

The system identification method is based on the asymptote approach [16] in three steps:

Step 1: Tracing the straight lines (asymptotes) and slopes. These asymptotes are just straight lines on the log vs. the log plot.

Step 2: Finding the break-points (pole and zero locations) arranged in the order of an increasing frequency. The two straight-line asymptotes capture the essential features of the plot meeting at a frequency corresponding to the pole or zero location. This is the "break-point".

Step 3: Finding the transfer functions corresponding to each straight line in order to construct the entire transfer function of the AC motor impedance.

Step 1: The straight lines are illustrated in Fig. 5. There are three asymptote lines, with three slopes:

1- At the frequencies of less than w_{n1}, then LF asymptote is -1.

2- For the frequencies between w_{n1} and w_{n2}, the MF asymptote is +1.

3- For the frequencies greater than w_{n2}, the HF asymptote is -1.

Step 2: The first observation coming from Fig.4 is that the CM impedance has two resonance frequencies, w_{n1} and w_{n2}, in the frequency range from 100 Hz to 30 MHz.

w_{n1} and w_{n2} are the natural frequencies of zeros and poles respectively of the Z_{CM} transfer function.

The order value of each zero and pole indicates the change in the slope. The slope is increased at zeros and reduced at poles [17].

Step 3: The left side of the graph shows that at LF when, $w < w1$, the slope of Z_{CM} magnitude plot is −1, thus corresponding to the integrator.

Therefore, the LF, asymptote ($w < w_{n1}$) is defined by the first term [3]:

$$Z_1 = \frac{K}{S} \qquad (11)$$

From w_1 to w_2, the slope of the Z_{CM} magnitude plot is +1; this change is from the second term defined by slope +2; the asymptote with slope +2 corresponding to the transfer function of the second-order system in the numerator can be given by relation :

$$Z_2 = (\frac{1}{w_1^2}) s^2 + \frac{2 \cdot \xi_1}{w_1} s + 1 \qquad (12)$$

w_1 is the first natural frequency of the Z_{CM} zeros.

ξ_1 is the Z_{CM} damping ratio.

For the frequencies greater than w_{n2}, the composite asymptote therefore decreases with slope -1. Each pole at the second natural frequency decreases the asymptotes with slopes -2 (+1 (the last slope)-2 (pole slope) = -1 (composite slope)).

The transfer function with slope -2 is of the second-order system in the denominator. It can be given by [3, 4]:

$$Z_3 = \frac{1}{\left[(\frac{1}{w_2^2}) s^2 + \frac{2 \cdot \xi_2}{w_2} s + 1 \right]} \qquad (13)$$

w_{n2} is the second natural frequency of the Z_{CM} poles.
ξ_2 is the Z_{CM} damping ratio.

Finally the entire Bode's log magnitude of Z_{CM} results from the superposition of all transfer functions at different frequencies. It can be written as:

$$Z_{CM} = Z_1 \cdot Z_2 \cdot Z_3 \qquad (14)$$

$$Z_{CM} = \frac{k \cdot \left[(\frac{1}{w_1^2}) s^2 + \frac{2 \cdot \xi_1}{w_1} s + 1 \right]}{s \cdot \left[(\frac{1}{w_2^2}) s^2 + \frac{2 \cdot \xi_2}{w_2} s + 1 \right]} \qquad (15)$$

The pole of the CM impedance in the origin; two complex conjugate zeros and two complex conjugate poles. The zeros and poles represent the break-points.

$$p_1 = 0 \qquad (16)$$

$$p_{2,3} = -w_{n2}\left(\zeta_2 \mp j\sqrt{1-\zeta_2^2}\right) \qquad (17)$$

$$z_{1,2} = -w_{n1}\left(\zeta_1 \mp j\sqrt{1-\zeta_1^2}\right) \qquad (18)$$

3.2 Identification of the transfer-function parameters

The constant terms "k" are located by passing through Z_{CM} at $w = 1$ even though the composite curve will not go through this point. So we can write:

$$-1 = \frac{\log(k) - \log(Z_0)}{\log(1) - \log(w_0)} \qquad (19)$$

w_{n1} is the first natural frequency of the Z_{CM} zeros. It corresponds to the first break-point, the meeting of the LF asymptote (slope -1) and the MF asymptote (slope +1) at a frequency corresponding to the w_{n1} (Fig. 6).

ξ_1 is the Z_{CM} damping ratio: we can find it by relation:

$$w_{p1} = w_{n1}\sqrt{1-\xi_1^2} \qquad (20)$$

w_{p1} is the damped natural frequency corresponding to the minimal value of the amplitude around first natural frequency w_{n1}.

w_{n2} is the second natural frequency of the Z_{CM} poles. It corresponds to the second break-point, the meeting point of the law and medium frequency asymptote

(slope +1) and the HF asymptote (slope-1) at a frequency corresponding to the w_{n2}.

ξ_2 is the Z_{CM} damping ratio found by relation:

$$w_{p2} = w_{n2}\sqrt{1-\xi_2^2} \qquad (21)$$

w_{p2} is the damped natural frequency corresponding to the maximal value of the amplitude around the second natural frequency w_{n2}.

Table. 1. Transfer-function parameters

Constant terms K	2.62005719e+09
The first natural frequency (w_{n1})	2.87688758e+05
(w_{p1}) damped natural frequency	2.81876265e+05
The second natural frequency (w_{n2})	4.16779364e+05
(w_{p2}) damped natural frequency	4.04598107e+05
The first damping ratio ξ_1	0.2
The second damping ratio ξ_2	0.24

The results confirm the Bode's plot of the magnitude of CM impedances Z_1, Z_2, Z_3, and Z_{CM} given by relations 12, 13, 14 and 16, respectively as shown in Fig. 5.
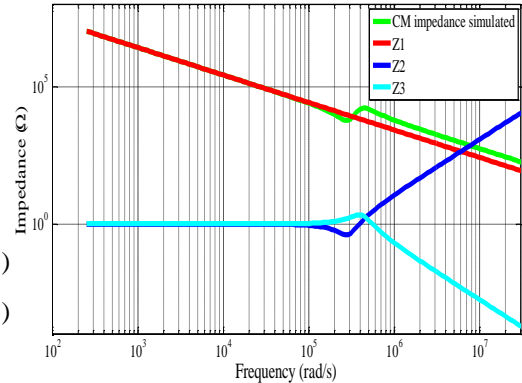

Figure 5. Simulated CM impedances.

Fig. 6 shows a comparison between the experimental and simulation results for the CM impedance.
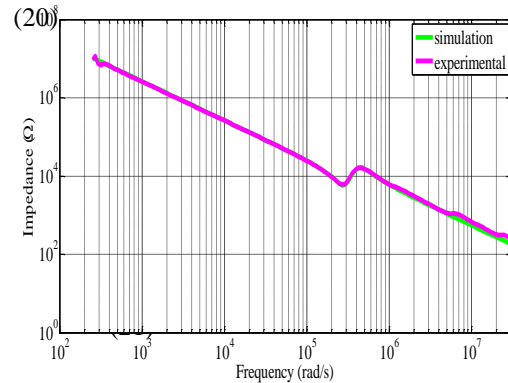

Figure 6. Comparison between the measured and simulated CM impedance.

As well seen, there is a good agreement between the experimental and simulation results obtained by the proposed approach.

The AC motor transfer function can be verified by using the second-phase angle plot. The Z_{CM} phase can be easily evaluated by:

$$\varphi_{Z_{CM}} = -90 + arctg\left(\frac{2 \cdot \xi_1 \cdot \frac{w}{w_1}}{1 - (\frac{w}{w_1})^2}\right) - arctg\left(\frac{2 \cdot \xi_2 \cdot \frac{w}{w_2}}{1 - (\frac{w}{w_2})^2}\right) \quad (22)$$

Fig. 7 shows the measurement result and the model data of the CM impedance phase of the AC motor.
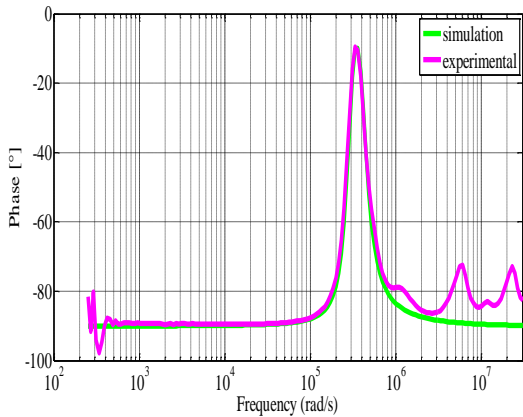

Figure 7. Comparison between the measured and simulated CM impedance (phase).

The best results are found on the frequency response of impedance Z_{CM} in the magnitude plot (Fig. 6). On the contrary, the frequency response of phase impedance Z_{CM} (Fig. 7) shows some discrepancy in the HF range.

4 ANALYSIS OF THE CM MOTOR IMPEDANCE

In the EMC studies, particularly for the inverter cable motor, the CM noise-current flows into the ground and through a stray capacitance inside the motor to the motor frame and back to the source via the power mains (Fig. 8).
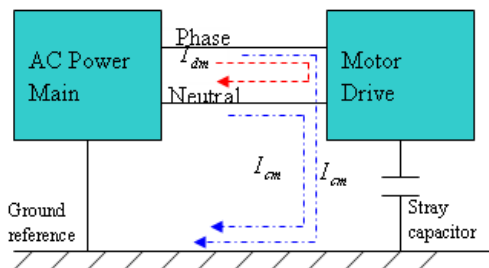

Figure 8. CM and DM current paths of the inverter cable motor.

So the path of the CM current is dominted by the parasite capacity existing between the motor windings and the ground.

The CM impedance of the motor can be represented by the impedance of this capacity in a HF range [5], as confirmed by the experimental and simulation results shown in Fig. 9.
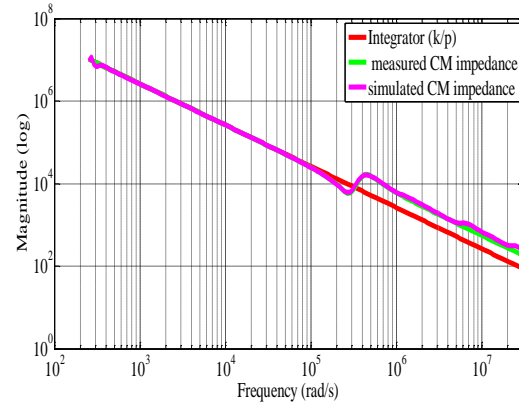

Figure 9. Comparison between the measured and simulated CM impedance and the integrator (magnitude).

The most of the LF and HF ranges, the magnitude decreases with slope -1, and the phase equals -90°. This plot corresponds to the Bode's plot of the integrator and also to the HF capacitance model. So the CM impedance of AC motor Z_{CM} is dominated by the capacity.

Above first resonant frequency w_{n1}, the impedance of the inductor and the impedance magnitude increase with slope +1.

As observed in Fig. 9, the CM impedance decreases as the switching frequency decreases. This is the reason why the CM currents are a serious problem at high switching-frequency drives [9].

As shown in Figs. 9 and 10, superimposing the experimental and simulation results of the proposed mathematical model demonstrates a very good accordance between them in terms of both the magnitude and phase.

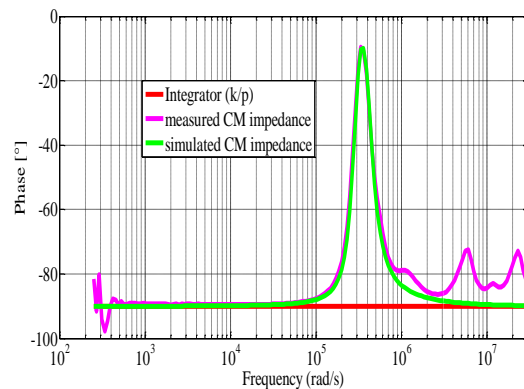Term Z_1 domintes the CM impedance of the AC motor an a LF and HF range.

Fig. 10. Comparison between the measured and simulated CM impedance and the integrator (phase).

5 CONCLUSION

In this paper, a HF model of a three-phase AC motor in a CM configuration is presented in the frequency range from 10 Hz up to 30 MHz based on the frequency-response method. The proposed model corresponds to the measurement results of both the magnitude and the phase.

The method can be used to predict and solve complex electrical systems in a HF range for the electromagnetic compatibility studies.

The CM impedance increases and the capacity between the motor and the ground dominates. This makes this parasitic capacity to be a preferred path for the CM currents and becomes a serious problem in high switching frequency drives.

To complete this work, the differential mode of the AC motor should be modelled.

REFERENCES

[1]   ] Mulyana, Tatang and Suhaimi, Farah Najaa and Hanafi, Dirman and Mohamad Nor, Mohd Than; " ARX Model of four types heat exchanger identification", In: Malaysian Technical Universities International Conference on Engineering and Technology (MUiCET'11), 13-15 November 2011, BatuPahat, Malaysia.

[2]   A. Boglietti, A. Cavagnino, M. Lazzari, "Experimental High Frequency Parameter Identification of AC Electrical Motors", IEEE Transactions on Industry Applications, Volume: 4, Issue: 1, pp. 23 – 29, Jan. 2007.

[3]   A.F. Moreira, T. A. Lipo, G. Venkataramanan, S Bernet, "High-frequency modeling for cable and induction motor overvoltage studies in long cable drives" , IEEE Transactions on Industry Applications, Vol.38, n.5, pp.1297-1306, September/October 2002.

[4]   YounggonRyu, Bo-Ryang Park ; Ki Jin Han, "Estimation of High-Frequency Parameters of AC Machine From Transmission Line Model", Magnetics, IEEE Transactions on (Volume: 51, Issue: 3) March 2015

[5]   L. Wang and J. Jatskevich, "High-Frequency Modeling for Cable and Induction Motor Overvoltage Studies in Long Cable Drives", Енергетика і автоматика, №3, 2013

[6]   A.Consoli, G.Oriti, A.Testa, A.L. Julian, "Induction Motor Modeling for Common Mode and Differential Mode Emission Evaluation", 1996 IEEE.

[7]   Christophe Vermaelen, « Contribution à la modélisation et à la réduction des perturbations conduites dans les systèmes d'entraînement à vitesse variable », Systèmes et Application des Technologies de l'Information et de l'Energie (SATIE) UMR CNRS 8029, these doctorat, école normale superieure de cachan, France 2003.

[8]   Bertrand Revol; James Roudet; Jean-Luc Schanen; Philippe Loizelet, "EMI Study of Three-Phase Inverter-Fed Motor Drives", vol. 47, no 1, p. 223-231, févr. 2011.

[9]   Stefan-Peter Weber, &kart Hoene, Stephan Guttowski, Werner John, Herbert Reichl, "Modeling Induction Machines for EMC-Analysis" , 2004 IEEE.

[10] Rao V.Dukkipati; "Analysis and Design of Control Systems Using Matlab", New Age International, Daryaganj.New.Delhi.2009.

[11] Joseph J. Distefano, Wan J. Williams, Allen R. Stubberud; "theory and problems of feedback and control systems", Second Edition. McGraw-Hill, 1995.

[12] Chung-Neng Huang, Chen-Min Cheng; A Novel Method of Transfer-Function Identification for Unknownsystems, Applied Mechanics and Materials Vols. 321-324 (2013) pp 1967-1970.

[13] Young-Sik Cho ; Daejeon, Korea ; Bok-Ryul Kim ; Hanju Cha, "Transfer function approach to a passive harmonic filter design for industrial process application" International Conference on Mechatronics and Automation (ICMA), August 4-7, 2010, Xi'an, China

[14] Y.Weens, N.Idir, J-J.Franchaud, R.Bausière, "Comparaison de deux méthodes de modélisation haute fréquence d'un moteur asynchrone", Colloque International de Compatibilité Electromagnétique, CEM'06, Saint Malo, France, pages. 187 – 189, 04/2006.

[15] YannickWeens, Nadir Idir, Jean-Jacques Franchaud, Robert Bausière, "High-Frequency Modeling of an Adjustable Speed Drive" IEEE Transactions on Electromagnetic Compatibility 51(3):665 - 672 • September 2009.

[16] James k.Phipps; A Transfer-Function Identification approach to harmonic design, Applied Mechanics and Materials Vols. 321-324 (2013) pp 1967-1970.

[17] H. Miloudi, A. Bendaoud, M. Miloudi, A. Gourbi, H. Slimani, "Common mode conducted electromagnetic interference in inverter fed-AC Motor", PRzeglądElektrotechniczny (Electrical Review), R. 86 NR 12/2010, pp.271-275, ISSN 0033-2097.

[18] H. Miloudi, A. Bendaoud, M. Miloudi, S. Dickmann, S. Schenke, "A Novel Method of Transfer-Function Identification for Modeling DM Impedance of AC Motor",*2017* International Symposium on Electromagnetic Compatibility – EMC, 04-08 september 2017, Angers, Frensh.

Houcine Miloudi is currently a Lecturer at the Institute of Electrical Engineering at the University of Sidi Bel-Abbès, Algeria. He has completed his PhD studies at the Djillali Liabes University. His research interests include electromagnetic compatibility in power converters, EMI reduction techniques, high-frequency power conversion, magnetic design and power electronics.

Abdelber Bendaoud is an Assistant Professor in at Institute of Electrical Engineering at the University of Sidi Bel-Abbès, Algeria. His research interests include electrostatic separation technologies, high-voltage insulation, gas discharges, electric and magnetic fields, and electromagnetic compatibility. He received his PhD degree from the University of Djilali Liabes of Sidi Bel-Abbès.

Mohamed Miloudi is a graduate student and a graduate Assistant at the Ahmed Zabana University Center, Algeria. He is pursuing his PhD studies in Electrical Engineering. His research interests include electromagnetic compatibility, system identification, and electronic power converters.